RSC Advances

ROYAL SOCIETY OF CHEMISTRY

www.rsc.org/advances

Organotin(IV) carboxylate derivatives as a new addition to anticancer and antileishmanial agents: Design, physicochemical characterization and interaction with Salmon sperm DNA

Muhammad Sirajuddin[a,*], Saqib Ali[b,*], Vickie McKee[c], Sumera Zaib[d], Jamshad Iqbal[d]

[a] Department of Chemistry, COMSATS Institute of Information Technology, Abbottabad, 22060, Pakistan

[b] Department of Chemistry, Quaid-i-Azam University, Islamabad 45320, Pakistan

[c] Department of Chemistry, Loughborough University, Loughborough, Leics LE11 3TU, UK

[d] Centre for Advanced Drug Research, COMSATS Institute of Information Technology, Abbottabad, 22060, Pakistan

*Corresponding author addresses:

m.siraj09@yahoo.com (M. Sirajuddin); drsa54@hotmail.com (S. Ali), Tel.: +92-51-90642130; Fax: +92-51-90642241

Abstract

This article emphasizes on the synthesis, characterization of novel organotin(IV) carboxylate complexes and their application on medicinal side. Metal complexes and organometallic compounds have a growing importance in medicine, particularly in oncology. Organotin derivatives have caught much attention during the last two decades for their potential biocidal activities. In recent years several organotin compounds have been synthesized, some with interesting cytotoxic properties. Here we will focus on the relevance of organotin derivatives as very promising potential candidates in anticancer therapy. Ten new organotin(IV) complexes were synthesized and characterized by using FT-IR, NMR (^{1}H, ^{13}C and ^{119}Sn), elemental analysis, mass spectrometry and single crystal X-ray techniques. Results of the infrared spectroscopy of the sodium salt and complexes showed that the coordination took place through oxygen atoms of the carboxylate group. Crystallographic data for complexes **1** and **3** showed the tin has a distorted trigonal bipyramidal geometry with the three alkyl groups in the trigonal plane while the two oxygen atoms in the equatorial plane. In case of complex **4** the geometry is tetrahedral due to the steric hindrance of the bulky phenyl groups. The compounds were screened for *in vitro* antiproliferative activity against lung carcinoma (H-157) and kidney fibroblast (BHK-21) cell lines and revealed significant anticancer activity. They were also tested for *antileishmanial* activity against the promastigote form of leishmania major and exhibited IC_{50}

value 0.98 ± 0.06 μM as compared to amphotericin B (IC_{50} value 0.29 ± 0.05 μM). The synthesized compounds act as a potent intercalator of SS-DNA and insert themselves into the nitrogenous bases of the DNA resulting in hypochromism and bathochromic shift.

Keywords: Carboxylate ligand; Organotin(IV) complex; Anticancer activity; Antileishmanial activity; DNA interaction

1. Introduction

The use of metal complexes as chemotherapeutic agents in the treatment of illness, which is a major public health concern, appears as a very attractive alternative. The achievement of *cis*-platin for the treatment of testicular and ovarian cancer attracted the researcher concentration to other metal-based antineoplastic agents. Metal-based compounds are of particular interest due to their physical and chemical properties. Properties such as ligand exchange rates, redox properties, oxidation states, coordination affinities, solubility, biodisponibility, and biodistribution could be modified in order to enhance the therapeutic effect while plummeting the side effects.[1] One approach that could produce successful results involves the metal coordination of ligands with well-known biological activity. In this way, the designed metal-based compound combines ligands with an important biological activity and pharmacologically active metals in a single chemical moiety. This strategy could produce enhanced efficiency and reduced toxic or side effects while lowering the therapeutic doses and/or overcoming drug resistance mechanisms. Additionally the metal could act as a carrier and/or stabilizer of the drug until it is able to reach the target. At the same time, the organic ligand with well-known biological activity could transport and protect the metal, then avoiding side reactions on its route to the potential targets. The metal-ligand combined effects may result in an important improvement in the activity of the resulting coordination compounds.[1-3]

Cancer chemotherapy based on metal complexes has gained momentum after the serendipitous discovery of *cis*-platin, and remains a front line treatment for most aggressive solid tumors.[4] Therefore, novel treatments are urgently needed for cancer therapy. The fight against cancer is the main and primary target concerning this research. The initial efforts in the evaluation of platinum-based anticancer drugs have been shifted to non-platinum metal-based agents.[5] Thus, an intensive study of other metals (Ti, Ga, Ge, Pd, Au, Co, Ru and Sn) is being carried out and is helping to improve the problems associated with the use of platinum compounds as anticancer

drugs.[6] Recent studies have shown very promising *in vitro* antitumor properties of organotin compounds against a wide panel of tumor cell lines of human origin.[7] In some cases, organotin(IV) derivatives have also shown acceptable antiproliferative *in vivo* activity as new chemotherapy agents.[8]

Leishmaniasis has been defined by the World Health Organization as a group of diseases that severely affects 12 million people residing in the warm areas of the world.[9] In most of the cases, patients cannot survive if proper treatment is not provided during development of this sand fly mediated parasitic disease. Several *antileishmanial* agents have already been reported[10,11] but none of these proved to be the ultimate choice of drug due to varying degrees of efficacy and toxicity. Among these, pentavalent antimonials although are recognized to be the most useful drug for treatment of visceral leishmaniasis caused by *Leishmania donovani*[12], discovery of antimony salt resistant pathogenic strains has made the situation worse to treat the patients against these parasites.[13] Miltefosine, an orally active phosphocholine analogue, also appeared to be effective in the treatment of the disease.[14] However, still there is a need to identify new chemotherapeutic agents for effective therapy of the visceral form of *leishmaniasis*, commonly abbreviated as kala-azar.[15]

In continuation to our previous research work, we are reporting here the synthesis and biological applications of organotin(IV) carboxylate derivatives of N-[(2-methoxy-5-nitrophenyl)]-4-oxo-4-[oxy]butanamide. All the synthesized compounds were successfully characterized by FT-IR, multi NMR (^{1}H, ^{13}C, ^{119}Sn), elemental analysis (CHN), mass spectrometry and single crystal X-ray analysis. They were tested for *in vitro* antiproliferative and antileishmanial activities and got excellent results.

2. Experimental section

2.1. Materials and methods

Reagents Me_3SnCl, *n*-Bu_3SnCl, Ph_3SnCl, Cy_3SnCl, Me_2SnCl_2, *n*-Bu_2SnCl_2, *tert*-Bu_2SnCl_2, Ph_2SnCl_2, *n*-Oct_2SnO, 2-methoxy-5-nitroaniline, succinic anhydride were obtained from Aldrich (USA) and were used without further purification. All the solvents purchased from E. Merck (Germany) were dried before use according to the literature procedures.[16] Sodium salt of Salmon sperm DNA (SS-DNA) (Arcos) was used as received. The melting points were determined in a capillary tube using a Gallenkamp (UK) electrothermal melting point apparatus. IR spectra in

the range of 4000-100 cm^{-1} were obtained on a Thermo Nicolet-6700 FT-IR Spectrophotometer equipped with DTGS (deuterated triglycine sulphate) detector. Elemental analysis was done using a CE-440 Elemental Analyzer (Exeter Analytical, Inc) and the experimentally found values are given in parenthesis in experimental part. ^{1}H, ^{13}C and ^{119}Sn NMR were recorded on a 400 MHz JEOL ECS instrument, using DMSO as an internal reference [^{1}H (DMSO-d6) = 2.50 ppm and ^{13}C (DMSO-d6) = 39.5 ppm]. For ^{119}Sn NMR the measurement was recorded at a working frequency of 37.718749 MHz. Chemical shifts are given in ppm and coupling constants (*J*) values are given in Hz. The multiplicities of the signals in ^{1}H NMR are given with chemical shifts; (s = singlet, d = doublet, t = triplet, q = quartet, m = multiplet, dd = doublet of a doublet). The absorption spectra were measured on a Shimadzu 1800 UV-visible Spectrophotometer. X-ray data for complexes **3** and **4** were collected at 150 (2) K on a Bruker Apex II CCD diffractometer. Details are given in Table 2. All the non-hydrogen atoms were refined using anisotropic atomic displacement parameters, and hydrogen atoms bonded to carbon were inserted at calculated positions using a riding model. Hydrogen atoms bonded to O or N were located from difference maps and their coordinates refined. SHELXS-97[17] was used to solve and SHELX2012[18] to refine the structures. The mass spectra were recorded on a Thermo Scientific executive (orbitrap) utilizing an Advion TriVersa ^{TM}NanoMate sample introduction system. The m/z values were evaluated assuming that H = 1, C = 12, N = 14, O = 16, Cl = 35, and Sn = 120.

2.2. Synthesis

Synthesis of sodium salt of Ligand: Sodium N-[(2-methoxy-5-nitrophenyl)]-4-oxo-4-[oxy]butanamide (NaL)

An aqueous solution of sodium hydrogen carbonate ($NaHCO_3$) was added to a suspended solution of the ligand, N-[(2-methoxy-5-nitrophenyl)]-4-oxo-4-[oxy]butanamide, in distilled water. The mixture was stirred at room temperature to get a clear solution which was then rotary evaporated to get the desired sodium salt of the ligand.[19] The chemical reaction is shown in Scheme 1.

IR (4000-400 cm^{-1}): 3357 ν (NH); 1680 ν (amide C=O); 1537 ν (COOasym); 1259 ν (COOsym); 278 (Δν).

Synthesis of organotin(IV) complexes

Organotin(IV) carboxylates were synthesized by refluxing a mixture of R_3SnCl (5 mmol)/ R_2SnCl_2 (2.5 mmol) and the sodium salt of ligand **NaL** (5 mmol) in dry toluene for 8 h (Scheme 1).[19] The refluxed solution was kept for overnight at room temperature. The NaCl precipitate was removed by filtration and the solvent was removed under the reduced pressure. The product was purified by recrystallization from chloroform at room temperature. The numbering of the ligand, N-[(2-methoxy-5-nitrophenyl)]-4-oxo-4-[oxy]butanamide (HL), and alkyl groups attached to Sn is given in Scheme 2.

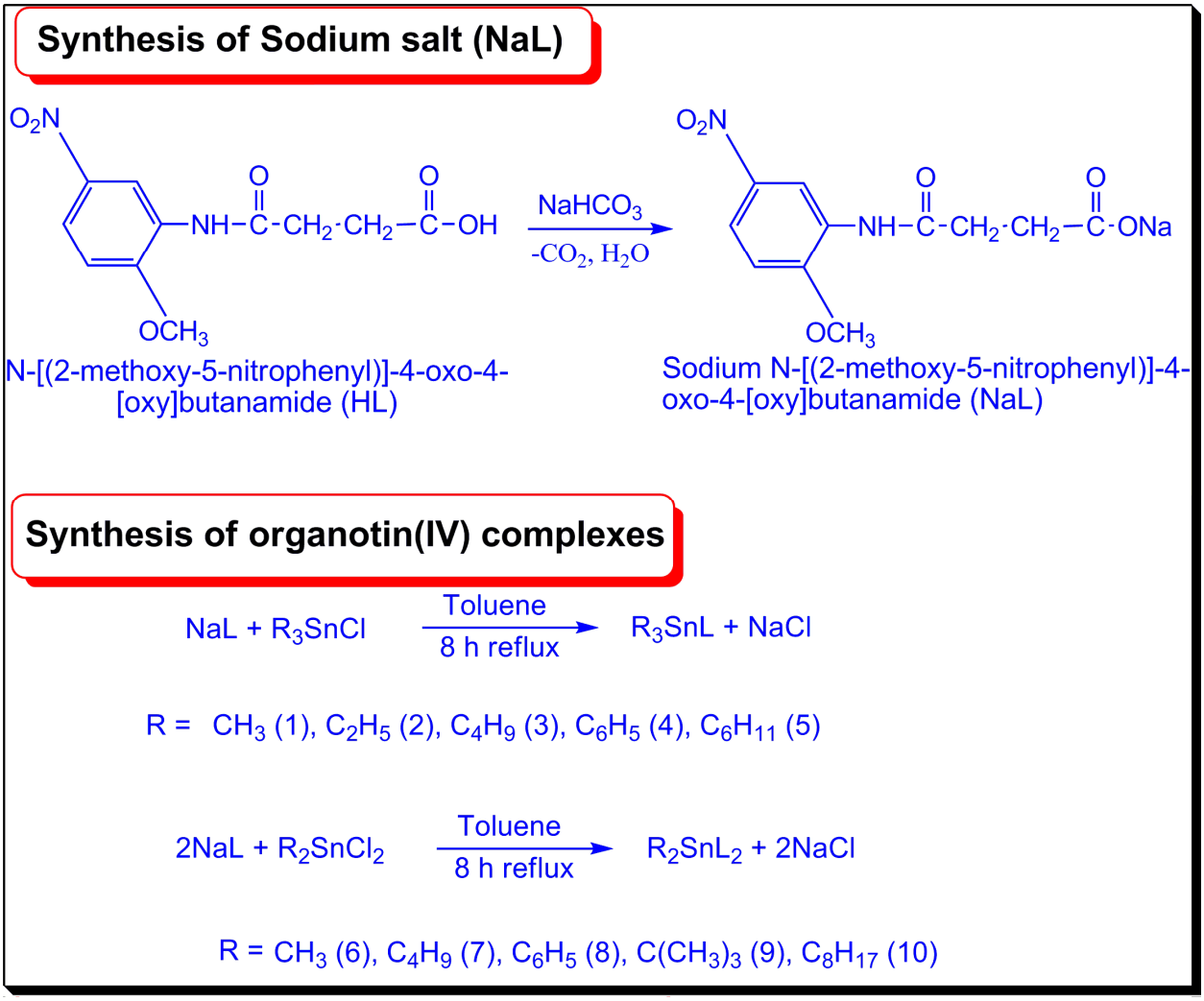

Scheme 1: Systematic route for the synthesis of NaL and organotin(IV) complexes

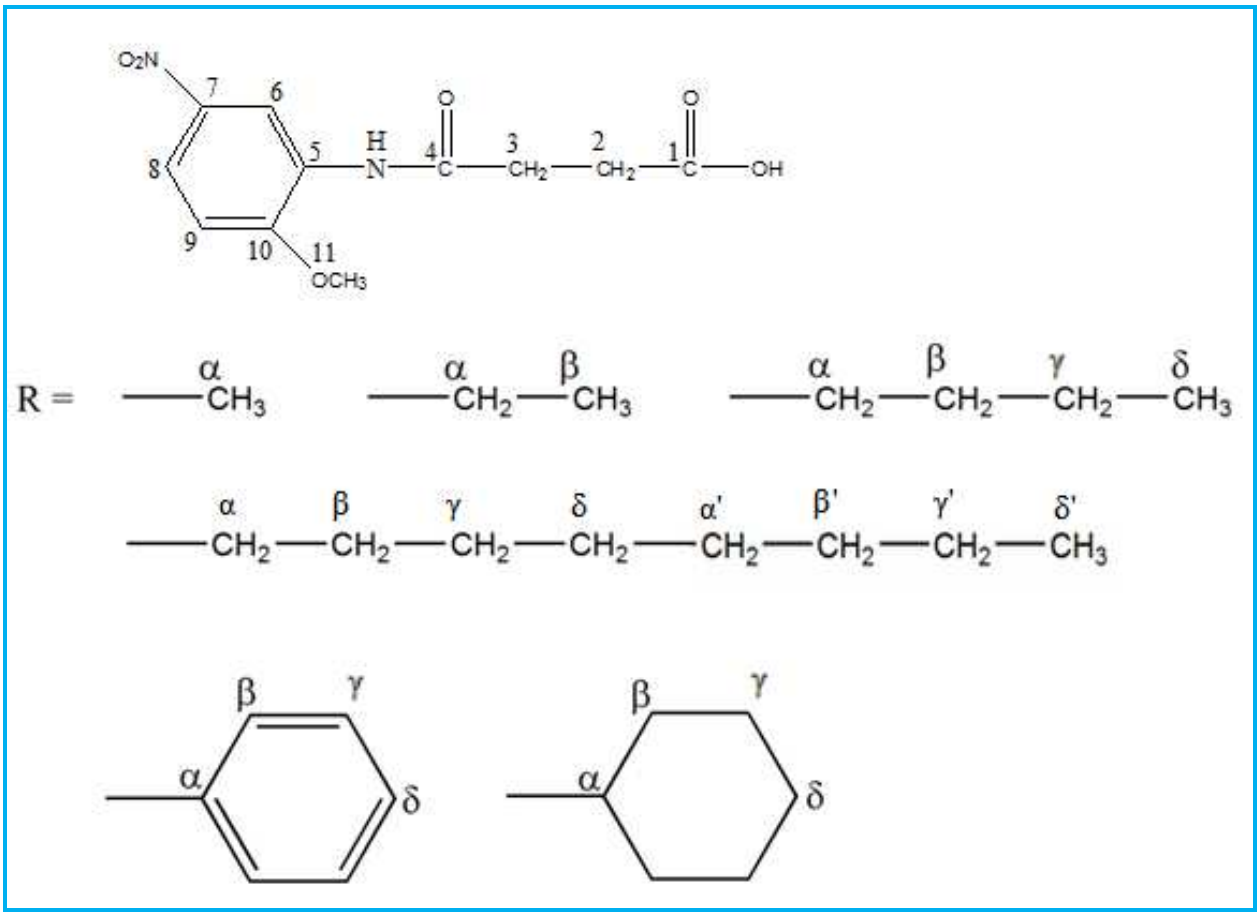

Scheme 2: Numbering pattern for HL and organic moieties attached to Sn atom

Trimethylstannyl 4-(4-methoxy-2-nitrophenylamino)-4-oxobutanoate (1)

Yield: 85%: M.p. 172-174°C: Mol. Wt.: 431.0: Anal. Calc. for $C_{14}H_{20}N_2O_6Sn$: C, 39.0 (38.8); H, 4.7 (4.8); N, 6.3 (5.9): **IR** (4000-400 cm^{-1}): 3358 ν (NH); 1691 ν (amide C=O); 1526 ν (COOasym); 1366 ν (COOsym); 160 (Δν); 550 ν (Sn-C); 461 ν (Sn-O): **^{1}H NMR** (DMSO-d6, 400 MHz) δ (ppm): 2.55 (t, 2H, H2, $^3J[^1H, ^1H]$ = 6.8 Hz); 2.32 (t, 2H, H3, $^3J[^1H, ^1H]$ = 6.8 Hz); 9.47 (s, 1H NH); 8.98 (d, 1H, H6, $^4J[^1H, ^1H]$ = 2.8 Hz); 7.98 (dd, 1H, H8, $^4J[^1H, ^1H]$ = 2.8 Hz); 7.21 (d, 1H, H9, $^3J[^1H, ^1H]$ = 9.2 Hz); 3.94 (s, 3H, H11); 0.32 (s, 3H, Hα, $^2J[^{119}Sn\text{-}^1H\alpha]$ = 69 Hz): **^{13}C NMR** (DMSO-d6, 100 MHz) δ (ppm): 172.5 (C1); 33.1 (C2); 31.5 (C3); 176.4 (C4); 128.6 (C5); 111.4 (C6); 140.8 (C7); 115.8 (C8); 120.4 (C9); 154.6 (C10); 57.2 (C11); 0.7 (Cα, $^1J[^{119}Sn\text{-}^{13}C\alpha$ = 520 Hz): **^{119}Sn NMR** (DMSO-d6, 400 MHz) δ (ppm): -10.8: **ESI-MS**, m/z (%): $[C_{14}H_{20}N_2O_6SnNa]^+$, m/z = 455 (51.4); $[C_{14}H_{20}N_2O_6Sn]^+$, m/z = 432 (28); $[C_{11}H_{11}O_6N_2]^+$, m/z = 267 (3); $[C_{10}H_{11}N_2O_4]^+$, m/z = 223 (2); $[C_3H_9Sn]^+$, m/z = 165 (100); $[C_2H_6Sn]^+$, m/z = 150 (2);

$[CH_3Sn]^+$, m/z = 135 (32); $[Sn]^+$, m/z = 120 (13); $[C_{13}H_{17}N_2O_6Sn]^+$, m/z = 417 (5); $[C_{12}H_{17}N_2O_4Sn]^+$, m/z = 373 (24); $[C_{11}H_{14}N_2O_4Sn]^+$, m/z = 358 (31); $[C_{10}H_{11}N_2O_4Sn]^+$, m/z = 343 (70).

Triethylstannyl 4-(4-methoxy-2-nitrophenylamino)-4-oxobutanoate (2)

Yield: 80%: M.p. 124-126°C: Mol. Wt.: 473.1: Anal. Calc. for $C_{17}H_{26}N_2O_6Sn$: 43.0 (43.0); H, 5.5 (5.5); N, 5.9 (5.7): **IR** (4000-400 cm^{-1}): 3419 ν (NH); 1734 ν (amide C=O); 1520 ν (COOasym); 1365 ν (COOsym); 155 (Δν); 546 ν (Sn-C); 486 ν (Sn-O): **^{1}H NMR** (DMSO-d6, 400 MHz) δ (ppm): 2.54 (t, 2H, H2, $^3J[^1H, ^1H]$ = 6.8 Hz); 2.33 (t, 2H, H3, $^3J[^1H, ^1H]$ = 6.8 Hz); 9.50 (s, 1H NH); 8.97 (d, 1H, H6, $^3J[^1H, ^1H]$ = 9.2 Hz); 7.98 (dd, 1H, H8, $^4J[^1H, ^1H]$ = 2.8 Hz); 7.23 (d, 1H, H9, $^4J[^1H-^1H]$ = 2.8 Hz); 3.93 (s, 3H, H11); 1.02 (q, 2H, Hα, $^2J[^{119/117}Sn-^1Hα]$ = 76, 74 Hz); 1.20 (t, 3H, Hβ, $^3J[^1H, ^1H]$ = 8.0 Hz): **^{13}C NMR** (DMSO-d6, 100 MHz) δ (ppm): 172.4 (C1); 33.0 (C2); 31.2 (C3); 176.4 (C4); 128.5 (C5); 111.4 (C6); 140.8 (C7); 115.8 (C8); 120.3 (C9); 154.5 (C10); 57.1 (C11); 11.1 (Cα, $^1J[^{119}Sn-^{13}Cα]$ = 580 Hz); 10.5 (Cβ, $^2J[^{119}Sn-^{13}Cβ]$ = 34 Hz): **^{119}Sn NMR** (DMSO-d6, 400 MHz) δ (ppm): -16.2: **ESI-MS**, m/z (%): $[C_{17}H_{26}N_2O_6SnNa]^+$, m/z = 497 (30); $[C_{17}H_{26}N_2O_6Sn]^+$, m/z = 432 (15); $[C_{11}H_{11}N_2O_6]^+$, m/z = 267 (34); $[C_{10}H_{11}N_2O_4]^+$, m/z = 223 (13); $[C_6H_{15}Sn]^+$, m/z = 207 (100); $[C_4H_{10}Sn]^+$, m/z = 178 (35); $[C_2H_5Sn]^+$, m/z = 149 (40); $[Sn]^+$, m/z = 120 (35); $[C_{15}H_{21}N_2O_6Sn]^+$, m/z = 445 (16); $[C_{14}H_{21}N_2O_4Sn]^+$, m/z = 401 (11); $[C_{12}H_{16}N_2O_4Sn]^+$, m/z = 372 (13); $[C_{12}H_{16}N_2O_4]^+$, m/z = 252 (15).

Tributylstannyl 4-(4-methoxy-2-nitrophenylamino)-4-oxobutanoate (3)

Yield: 85%: M.p. 115-117°C: Mol. Wt.: 557.3: Anal. Calc. for $C_{23}H_{38}N_2O_6Sn$: C, 49.6 (48.1); H, 6.9 (7.3); N, 5.0 (4.9): **IR** (4000-400 cm^{-1}): 3358 ν (NH); 1738 ν (amide C=O); 1526 ν (COOasym); 1373 ν (COOsym); 153 (Δν); 540 ν (Sn-C); 489 ν (Sn-O): **^{1}H NMR** (DMSO-d6, 400 MHz) δ (ppm): 2.56 (t, 2H, H2, $^3J(^1H, ^1H)$ = 6.4 Hz); 2.34 (t, 2H, H3, $^3J[^1H, ^1H]$ = 6.4 Hz); 9.43 (s, 1H NH); 9.03 (d, 1H, H6, $^4J[^1H, ^1H]$ = 2.8 Hz); 7.95 (dd, 1H, H8, $^4J[^1H, ^1H]$ = 2.8 Hz); 7.20 (d, 1H, H9, $^3J[^1H, ^1H]$ = 9.2 Hz); 3.93 (s, 3H, H11); 0.99 (t, 2H, Hα, $^3J[^1H, ^1H]$ = 8.0 Hz); 1.53 (m, 2H, Hβ); 1.26 (m, 2H, Hγ); 0.79 (t, 3H, Hδ, $^3J[^1H, ^1H]$ = 7.2 Hz): **^{13}C NMR** (DMSO-d6, 100 MHz) δ (ppm): 172.4 (C1); 33.2 (C2); 31.4 (C3); 176.4 (C4); 128.8 (C5); 111.2 (C6); 140.8 (C7); 115.6 (C8); 120.2 (C9); 154.4 (C10); 57.1 (C11); 21.4 (Cα, $[^{119}Sn-^{13}Cα]$ = 384 Hz); 28.2 (Cβ, $[^{119}Sn-^{13}Cβ]$ = 27 Hz); 27.0 (Cγ, $[^{119}Sn-^{13}Cγ]$ = 75 Hz); 14.1 (Cδ): **^{119}Sn NMR**

(DMSO-d6, 400 MHz) δ (ppm): -17.3: **ESI-MS**, m/z (%): $[C_{23}H_{38}N_2O_6SnNa]^+$, m/z = 581 (5); $[C_{23}H_{38}N_2O_6Sn]^+$, m/z = 558 (15); $[C_{11}H_{11}N_2O_6]^+$, m/z = 267 (5); $[C_{10}H_{11}N_2O_4]^+$, m/z = 223 (10); $[C_{12}H_{27}Sn]^+$, m/z = 291 (100); $[C_8H_{18}Sn]^+$, m/z = 234 (35); $[C_4H_9Sn]^+$, m/z = 177 (25); $[Sn]^+$, m/z = 120 (10); $[C_{19}H_{29}N_2O_6Sn]^+$, m/z = 501 (11); $[C_{18}H_{29}N_2O_4Sn]^+$, m/z = 457 (41); $[C_{14}H_{20}N_2O_4Sn]^+$, m/z = 400 (12); $[C_{14}H_{20}N_2O_4Sn]^+$, m/z = 343 (23).

Triphenylstannyl 4-(4-methoxy-2-nitrophenylamino)-4-oxobutanoate (4)

Yield: 85%: M.p. 161-163°C: Mol. Wt.: 617.2: Anal. Calc. for $C_{29}H_{26}N_2O_6Sn$: C, 56.4 (55.6); H, 4.3 (4.2); N, 4.5 (4.0): **IR** (4000-100 cm^{-1}): 3306 ν (NH); 1739 ν (amide C=O); 1536 ν (COOasym); 1324 ν (COOsym); 212 (Δν); 541 ν (Sn-C); 439 ν (Sn-O): **^{1}H NMR** (DMSO-d6, 400 MHz) δ (ppm): 2.53 (t, 2H, H2, $^3J[^1H, ^1H]$ = 6.4 Hz); 2.35 (t, 2H, H3, $^3J[^1H, ^1H]$ = 6.4 Hz); 9.42 (s, 1H NH); 9.01 (d, 1H, H6, $^4J[^1H, ^1H]$ = 2.8 Hz); 7.98 (dd, 1H, H8, $^4J[^1H, ^1H]$ = 3.2 Hz); 7.19 (d, 1H, H9, $^3J[^1H, ^1H]$ = 9.2 Hz); 3.98 (s, 3H, H11); 7.45 (d, 1H, Hβ, $^3J[^1H, ^1H]$ = 6.4 Hz); 7.81 (m, 1H, Hγ); 7.34 (m, 1H, Hδ): **^{13}C NMR** (DMSO-d6, 100 MHz) δ (ppm): 172.2 (C1); 32.9 (C2); 31.5 (C3); 176.2 (C4); 128.9 (C5); 111.3 (C6); 140.8 (C7); 115.7 (C8); 120.3 (C9); 154.4 (C10); 57.1 (C11); 143.7 (Cα, $[^{119}Sn\text{-}^{13}C\beta]$ = 580 Hz); 136.7 (Cβ, $[^{119}Sn\text{-}^{13}C\beta]$ = 45 Hz); 128.7 (Cγ, $[^{119}Sn\text{-}^{13}C\gamma]$ = 61 Hz); 129.2 (Cδ): **^{119}Sn NMR** (DMSO-d6, 400 MHz) δ (ppm): 224.1, -257.5: **ESI-MS**, m/z (%): $[C_{29}H_{26}N_2O_6SnNa]^+$, m/z = 641 (6); $[C_{29}H_{26}N_2O_6Sn]^+$, m/z = 618 (19); $[C_{11}H_{11}N_2O_6]^+$, m/z = 267 (17); $[C_{10}H_{11}N_2O_4]^+$, m/z = 223 (10); $[C_{18}H_{15}Sn]^+$, m/z = 351 (100); $[C_{12}H_{10}Sn]^+$, m/z = 274 (35); $[C_4H_9Sn]^+$, m/z = 197 (25); $[Sn]^+$, m/z = 120 (20); $[C_{23}H_{21}N_2O_6Sn]^+$, m/z = 541 (21); $[C_{22}H_{21}N_2O_4Sn]^+$, m/z = 497 (34); $[C_{16}H_{16}N_2O_4Sn]^+$, m/z = 420 (28); $[C_{10}H_{11}N_2O_4Sn]^+$, m/z = 343 (34).

Tricyclohexylstannyl 4-(4-methoxy-2-nitrophenylamino)-4-oxobutanoate (5)

Yield: 83%: M.p. 129-131°C: Mol. Wt.: 635.4: Anal. Calc. for $C_{29}H_{44}N_2O_6Sn$: C, 54.8 (54.7); H, 7.0 (7.5); N, 4.4 (4.2): **IR** (4000-400 cm^{-1}): 3327 ν (NH); 1738 ν (amide C=O); 1531 ν (COOasym); 1365 ν (COOsym); 166 (Δν); 540 ν (Sn-C); 440 ν (Sn-O): **^{1}H NMR** (DMSO-d6, 400 MHz) δ (ppm): 2.61 (t, 2H, H2, $^3J[^1H, ^1H]$ = 6.4 Hz); 2.21 (t, 2H, H3, $^3J[^1H, ^1H]$ = 6.4 Hz); 9.48 (s, 1H NH); 9.07 (d, 1H, H6, $^4J[^1H, ^1H]$ = 2.8 Hz); 7.96 (dd, 1H, H8, $^4J[^1H, ^1H]$ = 2.8 Hz); 7.20 (d, 1H, H9, $^3J[^1H, ^1H]$ = 8.8 Hz); 3.94 (s, 3H, H11); 1.54 (t, 1H, Hα, $^3J[^1H, ^1H]$ = 6.4 Hz); 1.79 (m, 2H, Hβ); 1.50 (m, 2H, Hγ), 1.40 (m, 2H, Hδ): **^{13}C NMR** (DMSO-d6, 100 MHz) δ (ppm): 172.3 (C1); 33.1 (C2); 31.1 (C3); 176.8 (C4); 128.8 (C5); 111.2 (C6); 140.8 (C7); 115.5

(C8); 120.2 (C9); 154.4 (C10); 57.1 (C11); 27.1 (Cα, $^{1}J[^{119}Sn\text{-}^{13}C\alpha]$ = 599 Hz); 29.2 (Cβ, $^{2}J[^{119}Sn\text{-}^{13}C\beta]$ = 72 Hz); 31.1 (Cγ); 36.4 (Cδ): **^{119}Sn NMR** (DMSO-d6, 400 MHz) δ (ppm): -70.9: **ESI-MS**, m/z (%): $[C_{29}H_{44}N_2O_6SnNa]^+$, m/z = 659 (20); $[C_{29}H_{44}N_2O_6Sn]^+$, m/z = 636 (30); $[C_{11}H_{11}N_2O_6]^+$, m/z = 267 (18); $[C_{10}H_{11}N_2O_4]^+$, m/z = 223 (22); $[C_{18}H_{33}Sn]^+$, m/z = 369 (100); $[C_{12}H_{22}Sn]^+$, m/z = 287 (43); $[C_6H_{11}Sn]^+$, m/z = 197 (29); $[Sn]^+$, m/z = 120 (32); $[C_{23}H_{33}N_2O_6Sn]^+$, m/z = 553 (26); $[C_{22}H_{33}N_2O_4Sn]^+$, m/z = 509 (29); $[C_{16}H_{16}N_2O_4Sn]^+$, m/z = 426 (12); $[C_{10}H_{11}N_2O_4Sn]^+$, m/z = 343 (16).

Dimethylstannanediyl bis(4-(2-methoxy-5-nitrophenylamino)-4-oxobutanoate) (6)

Yield: 75%: M.p. 181-183°C: Mol. Wt.: 683.2: Anal. Calc. for $C_{24}H_{28}N_4O_{12}Sn$: C, 42.2 (42.1); H, 4.1 (4.0); N, 8.2 (8.0): **IR** (4000-400 cm^{-1}): 3351 ν (NH); 1738 ν (amide C=O); 1501 ν (COOasym); 1366 ν (COOsym); 135 (Δν); 539 ν (Sn-C); 464 ν (Sn-O): **^{1}H NMR** (DMSO-d6, 400 MHz) δ (ppm): 2.63 (t, 2H, H2, $^{3}J[^{1}H, ^{1}H]$ = 6.4 Hz); 2.47 (t, 2H, H3, $^{3}J[^{1}H, ^{1}H]$ = 6.4 Hz); 9.52 (s, 1H NH); 8.97 (d, 1H, H6, $^{4}J[^{1}H, ^{1}H]$ = 2.4 Hz); 7.97 (dd, 1H, H8, $^{4}J[^{1}H, ^{1}H]$ = 2.8 Hz); 7.21 (d, 1H, H9, $^{3}J[^{1}H, ^{1}H]$ = 9.2 Hz); 3.94 (s, 3H, H11); 0.73 (s, 3H, Hα, $[^{119}Sn\text{-}^{1}H\alpha]$ = 100 Hz): **^{13}C NMR** (DMSO-d6, 100 MHz) δ (ppm): 172.0 (C1); 32.2 (C2); 31.2 (C3); 174.5 (C4); 128.5 (C5); 111.4 (C6); 140.8 (C7); 115.9 (C8); 120.5 (C9); 154.6 (C10); 57.22 (C11); -0.1 (Cα, $^{1}J[^{119}Sn\text{-}^{13}C\alpha]$ = 800 Hz): **^{119}Sn NMR** (DMSO-d6, 400 MHz) δ (ppm): -303.7: **ESI-MS**, m/z (%): $[C_{24}H_{28}N_4O_{12}SnNa]^+$, m/z = 707 (80); $[C_{24}H_{28}N_4O_{12}Sn]^+$, m/z = 684 (25); $[C_{23}H_{25}N_4O_{12}Sn]^+$, m/z = 669 (6); $[C_{12}H_{14}N_2O_6Sn]^+$, m/z = 402 (12); $[C_{11}H_{11}N_2O_6Sn]^+$, m/z = 387 (12); $[C_{11}H_{11}N_2O_6]^+$, m/z = 267 (32); $[C_{10}H_{11}N_2O_4]^+$, m/z = 223 (23); $[C_2H_6Sn]^+$, m/z = 150 (10); $[CH_3Sn]^+$, m/z = 135 (14); $[Sn]^+$, m/z = 120 (6); $[C_{13}H_{17}N_2O_6Sn]^+$, m/z = 417 (100); $[C_{12}H_{17}N_2O_4Sn]^+$, m/z = 373 (17); $[C_{11}H_{14}N_2O_4Sn]^+$, m/z = 358 (20); $[C_{10}H_{11}N_2O_4Sn]^+$, m/z = 343 (17); $[C_{22}H_{25}N_4O_{10}Sn]^+$, m/z = 625 (8).

Dibutylstannanediyl bis(4-(2-methoxy-5-nitrophenylamino)-4-oxobutanoate) (7)

Yield: 84%: M.p. 149-151°C: Mol. Wt.: 767.4: Anal. Calc. for $C_{30}H_{40}N_4O_{12}Sn$: C, 46.9 (46.2); H, 5.2 (5.5); N, 7.3 (7.5): **IR** (4000-400 cm^{-1}): 3300 ν (NH); 1738 ν (amide C=O); 1504 ν (COOasym); 1366 ν (COOsym); 138 (Δν); 538 ν (Sn-C); 439 ν (Sn-O): **^{1}H NMR** (DMSO-d6, 400 MHz) δ (ppm): 2.65 (t, 2H, H2, $^{3}J[^{1}H, ^{1}H]$= 6.4 Hz); 2.46 (t, 2H, H3, $^{4}J[^{1}H, ^{1}H]$ = 6.4 Hz); 9.01 (s, 1H NH); 7.96 (d, 1H, H6, $^{4}J[^{1}H, ^{1}H]$ = 2.4 Hz); 7.23 (dd, 1H, H8, $^{4}J[^{1}H, ^{1}H]$ = 2.4 Hz); 7.21 (d, 1H, H9, $^{3}J[^{1}H, ^{1}H]$ = 9.2 Hz); 3.94 (s, 3H, H11); 1.18 (t, 2H, Hα, $^{3}J[^{1}H, ^{1}H]$ = 7.2 Hz);

1.43 (m, 2H, Hβ); 1.31 (m, 2H, Hγ); 0.74 (t, 3H, Hδ, $^{3}J[^{1}H, ^{1}H]$ = 7.2 Hz): **^{13}C NMR** (DMSO-d6, 100 MHz) δ (ppm): 171.9 (C1); 32.2 (C2); 31.2 (C3); 176.6 (C4); 128.6 (C5); 111.3 (C6); 140.8 (C7); 115.8 (C8); 120.4 (C9); 154.5 (C10); 57.2 (C11); 29.7 (Cα); 27.3 (Cβ); 26.2 (Cγ); 14.0 (Cδ): **^{119}Sn NMR** (DMSO-d6, 400 MHz) δ (ppm): -306.5: **ESI-MS**, m/z (%): $[C_{30}H_{40}N_4O_{12}SnNa]^+$, m/z = 791 (21); $[C_{30}H_{40}N_4O_{12}Sn]^+$, m/z = 768 (10); $[C_{26}H_{31}N_4O_{12}Sn]^+$, m/z = 711 (9); $[C_{15}H_{20}N_2O_6Sn]^+$, m/z = 444 (12); $[C_{11}H_{11}N_2O_6Sn]^+$, m/z = 387 (10); $[C_{11}H_{11}N_2O_6]^+$, m/z = 267 (8); $[C_{10}H_{11}N_2O_4]^+$, m/z = 223 (9); $[C_8H_{18}Sn]^+$, m/z = 234 (16); $[C_4H_9Sn]^+$, m/z = 177 (100); $[Sn]^+$, m/z = 120 (5); $[C_{19}H_{29}N_2O_6Sn]^+$, m/z = 501 (80); $[C_{18}H_{29}N_2O_4Sn]^+$, m/z = 457 (7); $[C_{14}H_{20}N_2O_4Sn]^+$, m/z = 400 (8); $[C_{10}H_{11}N_2O_4Sn]^+$, m/z = 343 (20); $[C_{25}H_{31}N_4O_{10}Sn]^+$, m/z = 667 (9).

Diphenylstannanediyl bis(4-(2-methoxy-5-nitrophenylamino)-4-oxobutanoate) (8)

Yield: 85%: M.p. 152-154°C: Mol. Wt.: 807.4: Anal. Calc. for $C_{34}H_{32}N_4O_{12}Sn$: C, 50.6 (50.9); H, 4.0 (4.4); N, 7.0 (6.9): **IR** (4000-100 cm^{-1}): 3304 ν (NH); 1738 ν (amide C=O); 1510 ν (COOasym); 1363 ν (COOsym); 147 (Δν); 538 ν (Sn-C); 440 ν (Sn-O): **^{1}H NMR** (DMSO-d6, 400 MHz) δ (ppm): 2.66 (t, 2H, H2, $^{3}J[^{1}H, ^{1}H]$ = 6.4 Hz); 2.48 (t, 2H, H3, $^{3}J[^{1}H, ^{1}H]$ = 6.4 Hz); 9.42 (s, 1H NH); 9.01 (d, 1H, H6, $^{4}J[^{1}H, ^{1}H]$ = 2.8 Hz); 7.98 (dd, 1H, H8, $^{4}J[^{1}H, ^{1}H]$ = 3.2 Hz); 7.19 (d, 1H, H9, $^{3}J[^{1}H, ^{1}H]$ = 9.2 Hz); 3.95 (s, 3H, H11); 7.29 (d, 1H, Hβ, $^{3}J[^{1}H, ^{1}H]$ = 6.4 Hz); 7.43 (m, 1H, Hγ); 7.12 (m, 1H, Hδ): **^{13}C NMR** (DMSO-d6, 100 MHz) δ (ppm): 171.3 (C1); 31.5 (C2); 29.3 (C3); 174.3 (C4); 128.6 (C5); 111.5 (C6); 140.8 (C7); 116.0 (C8); 120.6 (C9); 154.6 (C10); 57.2 (C11); 143.5 (Cα, $^{1}J[^{119}Sn\text{-}^{13}C\alpha]$ = 1236 Hz); 136.1 (Cβ); 128.1 (Cγ); 129.4 (Cδ): **^{119}Sn NMR** (DMSO-d6, 400 MHz) δ (ppm): -304.9: **ESI-MS**, m/z (%): $[C_{34}H_{32}N_4O_{12}SnNa]^+$, m/z = 831 (4); $[C_{34}H_{32}N_4O_{12}Sn]^+$, m/z = 808 (12); $[C_{28}H_{27}N_4O_{12}Sn]^+$, m/z = 731 (7); $[C_{17}H_{16}N_2O_6Sn]^+$, m/z = 464 (8); $[C_{11}H_{11}N_2O_6Sn]^+$, m/z = 387 (8); $[C_{11}H_{11}N_2O_6]^+$, m/z = 267 (11); $[C_{11}H_{11}N_2O_6]^+$, m/z = 269 (100); $[C_{10}H_{11}N_2O_4]^+$, m/z = 223 (13); $[C_{12}H_{10}Sn]^+$, m/z = 274 (21); $[C_6H_5Sn]^+$, m/z = 197 (230); $[Sn]^+$, m/z = 120 (8); $[C_{23}H_{21}N_2O_6Sn]^+$, m/z = 541 (90); $[C_{22}H_{21}N_2O_4Sn]^+$, m/z = 497 (11); $[C_{16}H_{16}N_2O_4Sn]^+$, m/z = 420 (21); $[C_{10}H_{11}N_2O_4Sn]^+$, m/z = 343 (30); $[C_{27}H_{27}N_4O_{10}Sn]^+$, m/z = 687 (21).

Di-*tert*-butylstannanediyl bis(4-(2-methoxy-5-nitrophenylamino)-4-oxobutanoate) (9)

Yield: 80%: M.p. 173-175°C: Mol. Wt.: 767.4: Anal. Calc. for $C_{30}H_{40}N_4O_{12}Sn$: C, 46.9 (45.6); H, 5.2 (5.3); N, 7.3 (7.1): **IR** (4000-400 cm^{-1}): 3360 ν (NH); 1739 (amide C=O); 1510 ν

(COOasym); 1366 ν (COOsym); 144 (Δν); 539 ν (Sn-C); 462 ν (Sn-O): **^{1}H NMR** (DMSO-d6, 400 MHz) δ (ppm): 2.70 (t, 2H, H2, $^{3}J[^{1}H, ^{1}H]$= 6.4 Hz); 2.57 (t, 2H, H3, $^{3}J[^{1}H, ^{1}H]$ = 6.4 Hz); 9.58 (s, 1H NH); 8.93 (d, 1H, H6, $^{4}J[^{1}H, ^{1}H]$ = 3.6 Hz); 7.98 (dd, 1H, H8, $^{4}J[^{1}H, ^{1}H]$ = 3.6 Hz); 7.21 (d, 1H, H9, $^{3}J[^{1}H, ^{1}H]$ = 6.8 Hz); 3.94 (s, 3H, H11); 1.23 (s, 9H, Hβ): **^{13}C NMR** (DMSO-d6, 100 MHz) δ (ppm): 171.7 (C1); 32.0 (C2); 30.6 (C3); 175.8 (C4); 128.4 (C5); 111.5 (C6); 140.8 (C7); 116.2 (C8); 120.6 (C9); 154.7 (C10); 57.2 (C11); 31.2 (Cα, $^{1}J[^{119}Sn-^{13}C\alpha]$ = 837 Hz); 29.9 (Cβ, $^{2}J[^{119}Sn-^{13}C\beta]$ = 133 Hz): **^{119}Sn NMR** (DMSO-d6, 400 MHz) δ (ppm): -292.1: **ESI-MS**, m/z (%): $[C_{30}H_{40}N_4O_{12}SnNa]^+$, m/z = 791 (55); $[C_{30}H_{40}N_4O_{12}Sn]^+$, m/z = 768 (30); $[C_{26}H_{31}N_4O_{12}Sn]^+$, m/z = 711 (22); $[C_{15}H_{20}N_2O_6Sn]^+$, m/z = 444 (13); $[C_{11}H_{11}N_2O_6Sn]^+$, m/z = 387 (16); $[C_{11}H_{11}N_2O_6]^+$, m/z = 267 (3); $[C_{11}H_{11}N_2O_6]^+$, m/z = 269 (40); $[C_{10}H_{11}N_2O_4]^+$, m/z = 223 (5); $[C_8H_{18}Sn]^+$, m/z = 234 (17); $[C_4H_9Sn]^+$, m/z = 177 (27); $[C_3H_6Sn]^+$, m/z = 162 (1); $[C_2H_3Sn]^+$, m/z = 147 (1); $[Sn]^+$, m/z = 120 (17); $[C_{19}H_{29}N_2O_6Sn]^+$, m/z = 501 (56); $[C_{18}H_{29}N_2O_4Sn]^+$, m/z = 457 (3); $[C_{14}H_{20}N_2O_4Sn]^+$, m/z = 400 (5); $[C_{10}H_{11}N_2O_4Sn]^+$, m/z = 343 (33); $[C_{25}H_{31}N_4O_{10}Sn]^+$, m/z = 667 (21).

Dioctylstannanediyl bis(4-(2-methoxy-5-nitrophenylamino)-4-oxobutanoate) (10)

Yield: 86%: M.p. 115-117°C: Mol. Wt.: 879.6: Anal. Calc. for $C_{38}H_{56}N_4O_{12}Sn$: C, 51.9 (51.8); H, 6.4 (6.4); N, 6.4 (6.2): **IR** (4000-400 cm^{-1}): 3304 ν (NH); 1736 (amide C=O); 1507 ν (COOasym); 1380 ν (COOsym); 127 (Δν); 538 ν (Sn-C); 455bν (Sn-O): **^{1}H NMR** (DMSO-d6, 400 MHz) δ (ppm): 2.66 (t, 2H, H2, $^{3}J[^{1}H, ^{1}H]$ = 6.0 Hz); 2.46 (t, 2H, H3, $^{3}J[^{1}H, ^{1}H]$ = 6.0 Hz); 9.51 (s, 1H NH); 9.0 (d, 1H, H6, $^{4}J[^{1}H, ^{1}H]$ = 2.8 Hz); 7.96 (dd, 1H, H8, $^{4}J[^{1}H, ^{1}H]$ = 2.8 Hz); 7.21 (d, 1H, H9, $^{3}J[^{1}H, ^{1}H]$ = 9.2 Hz); 3.94 (s, 3H, H11); 1.24 (t, 2H, Hα, $^{3}J[^{1}H, ^{1}H]$ = 6.8 Hz); 1.50 (bs, 6H, Hβ,γ,δ); 1.04 (b, 6H, Hα',β',γ'); 0.76 (t, 3H, Hδ', $^{3}J[^{1}H, ^{1}H]$ = 6.8 Hz): **^{13}C NMR** (DMSO-d6, 100 MHz) δ (ppm): 171.8 (C1); 33.2 (C2); 31.8 (C3); 177.9 (C4); 128.6 (C5); 111.4 (C6); 140.8 (C7); 115.8 (C8); 120.4 (C9); 154.5 (C10); 57.2 (C11); 24.9 (Cα); 29.5 (Cβ, $^{2}J[^{119}Sn-^{13}C\beta]$ = 17 Hz); 34.3 (Cγ); 29.2 (Cδ); 29.6 (Cδ); 29.1 (Cα'); 31.8 (Cβ'); 22.6 (Cγ'); 14.4 (Cδ'): **^{119}Sn NMR** (DMSO-d6, 400 MHz) δ (ppm): -271.7: **ESI-MS**, m/z (%): $[C_{38}H_{56}N_4O_{12}SnNa]^+$, m/z = 903 (33); $[C_{38}H_{56}N_4O_{12}Sn]^+$, m/z = 880 (2); $[C_{30}H_{39}N_4O_{12}Sn]^+$, m/z = 767 (1); $[C_{19}H_{28}N_2O_6Sn]^+$, m/z = 500 (2); $[C_{11}H_{11}N_2O_6Sn]^+$, m/z = 387 (2); $[C_{11}H_{11}N_2O_6]^+$, m/z = 267 (3); $[C_{10}H_{11}N_2O_4]^+$, m/z = 223 (4); $[C_{16}H_{34}Sn]^+$, m/z = 346 (3); $[C_8H_{17}Sn]^+$, m/z = 233 (2); $[Sn]^+$, m/z = 120 (1); $[C_{16}H_{34}]^+$, m/z = 226 (32); $[C_{15}H_{31}]^+$, m/z = 213 (100);

$[C_{27}H_{45}N_2O_6Sn]^+$, m/z = 613 (70); $[C_{26}H_{45}N_2O_4Sn]^+$, m/z = 569 (12); $[C_{18}H_{28}N_2O_4Sn]^+$, m/z = 456 (8); $[C_{10}H_{11}N_2O_4Sn]^+$, m/z = 343 (5); $[C_{29}H_{39}N_4O_{10}Sn]^+$, m/z = 723 (8).

Cell lines and cultures

Lung carcinoma (H-157), (ATCC CRL-5802) and kidney fibroblast (BHK-21), (ATCC CCL-10) cell lines were kept in RPMI-1640 [having heat-inactivated fetal bovine serum (10%) glutamine (2 mM), Pyruvate (1 mM), 100 U/mL penicillin and 100 µg/mL streptomycin] in T-75 cm^2 sterile tissue culture flasks in a 5% CO_2 incubator at 37°C.[20] 96-Well plates were used for growing H-157 and BHK-21 cells by inoculating 10^4 cells per 100 µL per well. For experiments, both cell lines were grown in 96-well plates by inoculating 10^4 and 5×10^4 cells/100 µL/well, respectively, and plates were incubated at 37°C in a 5% CO_2 incubator. Within 24 h, a uniform monolayer was formed which was used for experiments.

Cytotoxicity analysis by sulforhodamine B (SRB) assays: To perform cytotoxicity assay with H-157 and BHK-21 cells, a previously described method by Skehan *et al*.,[21] was adopted with some modifications. Briefly, cells were cultured in different 96 well plates for 24 h. The compounds in different concentrations (100, 10, 1 and 0.1 µM) were inoculated in test wells while control and blank wells were also prepared containing standard drug (Vincristine) and culture media with cells, respectively. The plates were then incubated for 48 h. After that cells were fixed with 50 µL of 50% ice cold trichloroacetic acid solution (TCA) at 4°C for 1 h. The plates were washed 5 times with phosphate-buffered saline (PBS) and air dried. Fixed cells were further treated with 0.4% w/v sulforhodamine B dye prepared in 1% acetic acid solution and left at room temperature for 30 min. After that the plates were rinsed with 1% acetic acid solution and allowed to dry. In order to solubilize the dye, the dried plates were treated with 10 mM Tris base solution for 10 min at room temperature. Absorbance was measured at 490 nm subtracting the background measurement at 630 nm.[22]

2.3. Antileishmanial activity

Parasite and culture: Leishmania major promastigotes were cultured at 25 ± 1°C to logarithmic phase in D-MEM/F-12 medium (Gibco BRL) without phenol red, supplemented by 10% heat inactivated fetal bovine serum (FBS), 100 IU/mL penicillin and 100 µg/mL streptomycin, then washed 3 times with PBS by centrifugation at 1500 rpm for 10 min at room temperature and resuspended at a concentration of 2.5×10^6 parasites/mL in medium.

Antileishmanial activity assays (MTT assay): The antileishmanial activity of the compounds was evaluated *in vitro* against the promastigote forms of Leishmania major using a MTT (3-(4,5-dimethylthiazol-2yl)-2,5-diphenyltetrazoliumbromide)-based microassay as a marker of cell viability. The MTT assay used was based on that originally described by Mosmann (1983)[23] modified by Niks and Otto (1990).[24] A stock solution of MTT (Sigma Chemical Co., St. Louis, Mo.) was prepared by dissolving in PBS at 5 mg/mL and storing in the dark at 4°C for up to 2 weeks before use. For the antileishmanial activity assays, 100 µL/well of the culture which contained 2.5×10^6 cells/mL promastigotes was seeded in 96-well flat-bottom plates. Then 10 µL/well from various concentrations of compounds were added to triplicate wells and plates were incubated for 72 h at 25 ± 1°C. The first well of 96 wells was as a blank well which only contained of 100 µL culture medium without any compound, drug or parasite. Amphotericin B was used as standard drug. At the end of incubation, 10 µL of MTT was added to each well and plates were incubated for 3 h at 25 ± 1°C. Enzyme reaction was then stopped by the addition of 100 µL of 50% isopropanol and 10% sodium dodecyl sulfate. The plates were incubated for an additional 30 min. under agitation at room temperature. Relative optical density (OD) was then measured at a wavelength of 570 nm using a 96-well microplate reader (Bio-Tek ELx 800TM, Instruments, Inc. USA). The background absorbance of plates was measured at 690 nm and subtract from 570 nm measurement. The absorbance of the formazan produced by the action of mitochondrial dehydrogenases of metabolically active cells is shown to correlate with the number of viable cells. All experiments were repeated at least three times. Results reported are mean of three independent experiments (± SEM) and expressed as percent inhibitions calculated by the formula:

$$\text{Inhibition (\%)} = \left[100 - \frac{\text{absorbance of the test compound}}{\text{absorbance of the control}}\right] \times 100$$

IC_{50} values of inhibitors were determined with the help of the Graph Pad prism 5.0 Software Inc., San Diego, California, USA.

2.4. DNA Interaction Study Assay By UV-Visible Spectroscopy

SS-DNA (50 mg) was dissolved by overnight stirring in deionized water (pH = 7.0) and kept at 4°C. Deionized water was used to prepare buffer (20 mM Phosphate buffer (NaH_2PO_4-Na_2HPO_4), pH = 7.2). A solution of (SS-DNA) in the buffer gave a ratio of UV absorbance at 260 and 280 nm (A_{260}/A_{280}) of 1.8, indicating that the DNA was sufficiently free of protein.[25,26]

The DNA concentration was determined *via* absorption spectroscopy using the molar absorption coefficient of 6,600 M^{-1} cm^{-1} (260 nm) for SS-DNA[27,28] and was found to be 1.4 $\times 10^{-4}$ M. The compound was dissolved in Ethanol at a concentration of 1 mM. The UV absorption titrations were performed by keeping the concentration of the compound fixed while varying the SS-DNA concentration. Equivalent solutions of SS-DNA were added to the complex and reference solutions to eliminate the absorbance of DNA itself. Compound-DNA solutions were allowed to incubate for about 10 min at room temperature before measurements were made. Absorption spectra were recorded using cuvettes of 1 cm path length at room temperature (25 ± 1°C).

3. Results and discussion

3.1. FT-IR

The IR spectra of the **NaL** and its organotin(IV) carboxylates were recorded using a Thermo Nicolet-6700 FT-IR Spectrophotometer in the range of 4000-400 cm^{-1} and comparison was made to assign the IR bands. The far-infrared spectra of Ph_3SnCl/Ph_2SnCl_2 derivatives were recorded in the range 400-100 cm^{-1}. Generally, ν (Sn-C) vibration bands for Ph-Sn complexes were observed in the far-infrared region (lower wavelength) compared to the ν (Sn-C) of dialkyltin(IV) or trialkyltin(IV) complexes which may be due to the mass effect of the Sn-Ph.[29] The detail of the FT-IR data of the synthesized ligand and its complexes are given in the experimental section.

FT-IR data of organotin(IV) derivatives reveal valuable information about the structure of the complexes in the solid state. The peaks of our interest are ν OH, ν NH, ν C=C, ν CO, ν Sn-C and ν Sn–O of the precursors and complexes.

The formation of the **NaL** was conform by FT-IR in which the OH peak at 3264 cm^{-1} was absent showing the displacement of H of **HL** with Na. **NaL** was then used for complexation as a starting material. Another important factor is Δν [ν (COOasym) – ν (COOsym)]. When there is interaction between the oxygen of the carboxylate group and tin, the asymmetric vibration ν (COOasym) decreases and the symmetric vibration ν (COOsym) increases, so the difference [Δν(COO)] decreases.[30] In the IR spectra of the **NaL** the ν (COOasym) appears at 1537 cm^{-1} and ν (COOsym) at 1259 cm^{-1}. While in complexes **1-10** the carboxylate bands are observed in the characteristic regions of 1536-1501 cm^{-1} for ν (COOasym) and 1380-1324 cm^{-1} for ν (COOsym). As reported that when the coordination changes from four to five or higher number, the ν

(COOasym) shifts to lower frequencies while ν (COOasym) shifts to higher frequencies, causing a decrease in the Δν value in compounds.[31] The magnitude of the Δν for the reported complexes is less than 200 cm^{-1} which reflects either chelating or bidentate nature of the ligand. The Δν value was also calculated from single crystal XRD data by using the following equation[32,33]:

$$\Delta\nu = 1818.1\delta r + 16.47(\theta OCO - 120) + 66.8$$

where δr is difference between the two C-O bond lengths (Å) and θOCO is the O-C-O angle (°).

A good correlation was found between the Δν value calculated from FT-IR data for complex **4** (212) and single crystal XRD data (216). In case of complex **3** the distances of C1-O1 and C1-O2 is same (1.258 Å) which means that the carboxylate moiety is symmetrically bridges the two Sn atoms.

Similarly the appearance of new peaks for ν (Sn-C) in the range of 550-538 cm^{-1} (for alkyl-Sn), 281-277 cm^{-1} (for phenyl-Sn) and for ν (Sn-O) in the range of 489-439 cm^{-1}, respectively confirms the synthesis of the new complexes.[34]

3.3. Multinuclear (^{1}H, ^{13}C and ^{119}Sn) NMR spectroscopy

NMR spectroscopy is one of the most widely used techniques for the characterization of organotin(IV) complexes. It is also helpful to predict the geometry of the complexes. The parameters $^{n}J(^{119}Sn,^{1}H)$, $^{n}J(^{119}Sn,^{13}C)$ and $\delta(^{119}Sn)$ are determined by this technique and afford the information about the geometry of the organotin(IV) complexes in solution state.

3.3.1. ^{1}H NMR spectroscopy

The ^{1}H and ^{13}C NMR spectra for the synthesized ligand and its complexes were recorded in DMSO using tetramethylsilane as an external standard and the data are given in the experimental section. The ^{1}H NMR spectrum of complex **1** (as a representative one) is shown in Fig. 1a. The ^{1}H NMR studies provide further support for the formation of compounds. The aliphatic protons at positions 2 (H2) and 3 (H3) appear as triplet with the ^{3}J bond coupling in all complexes. Protons 6 (H6) and 7 (H7) give doublet while proton 8 (H8) gives doublet of doublet. There is no significant change in the position of the NH signal in the spectra of the complexes indicating that nitrogen is not involved in coordination to tin.

According to the literature, coordination pattern of tin(IV) in di- and trimethyltin(IV) derivatives with the $^{1,2}J$ coupling constant values are a follow: in tetracoordinated tin compounds ($\theta \leq 112°$) ^{1}J values are predicted to be smaller than about 400 Hz, whereas ^{2}J values should be below 59

Hz; for pentacoordinated tin (θ = 115-130°), ^{1}J values fall in the range of 450-670 Hz and the ^{2}J values fall in the range of 65-80 Hz; finally, for hexacoordinated tin (θ = 129-176°) ^{1}J and ^{2}J values are generally larger than 670 and 83 Hz, respectively.[35,36] The methyl protons in trimethyltin(IV) complex (**1**) give a characteristic signal at 0.32 ppm with $^{2}J[^{119}\text{Sn-}^{1}\text{H}]$ = 69 Hz that falls in the range of 5-coordinate trigonal bipyramidal geometry around the tin atom in solution state.[37] The protons of triethyltin(IV) complex (**2**) give two peaks: a quartet for Hα with $^{2}J[^{119/117}\text{Sn-}^{1}\text{H}]$ = 76, 74 Hz and a triplet for Hβ. In the case of butyl proton (complex **3** and **7**) two triplets (one for Hα and one for Hδ) and two multiplets (one for Hβ and one for Hγ) were observed. The aromatic protons in Ph-Sn (complex **4** and **8**) appear as one doublet (Hβ) and two triplets (one for Hγ and one for Hδ). The protons of the cyclohexyl derivatives (complex **5**) generally give triplet for Hα, multiplet for Hβ and broad signals for Hγ and Hδ in the aliphatic regions. The methyl protons in the dimethyltin(IV) complex (**6**) give a signal at 0.73 ppm and $^{2}J[^{119}\text{Sn-}^{1}\text{H}]$ for dimethyltin(IV) derivatives were found to be 100 Hz that falls in the range of 6-coordinate octahedral geometry. The methyl protons of the *tertiary* butyl group in complex **9**, {$C(CH_3)_3$}, appear as a singlet at 1.23 ppm. In the case of octyltin(IV) complex (**10**), a somewhat different and complex pattern is observed for the methylene protons. The terminal protons give a triplet while the remaining protons give broad and complex signals. The observed $^{2}J[^{119}\text{Sn-}^{1}\text{H}]$ coupling constants for the methyl and ethlytin(IV) derivatives were used to calculate the C-Sn-C values while using the Lockhart's equation[38] and fall in the range of 5-coordinate trigonal bipyramidal geometry for the triorganotin(IV) derivatives and 6-coordinate octahedral geometry for the diorganotin(IV) derivatives. The values of C-Sn-C are given in Table 1.

3. 3.2. ^{13}C NMR spectroscopy

The detail of ^{13}C NMR data of the ligand and its organotin(IV) derivatives are given in the experimental section. The ^{13}C NMR spectra of complex **1** (as a representative one) are shown in Fig. 1b. The values were assigned to each carbon atom of the ligand and its complexes on the basis of incremental methods and by comparison with literature values.

The C=O resonances of the complexes were shifted downfield compared with the position in the free ligand. This downfield shift is due to the decrease of electron density at carbon atoms when oxygen is bonded to electropositive tin atom.[37] This observation provides further evidence that the complexation occurred through the oxygen atoms of the carboxylate group. However, the

signals for –C-N-, and -CH_2-CH_2- peaks for the alkyl as well as aryl groups attached to tin atom appeared in their specific regions.[39] The positions of the phenyl carbons of ligand undergo minor changes in the complex as compared to those observed in free ligand. The *ipso* carbon (Cα) of the phenyl group attached to tin atom appears in the range of 143.5-143.7 ppm that lies in the range of 5/6-coordination geometry.[40,41]

By substituting value of $^1J[^{119}Sn\text{-}^{13}C]$ in the Lockhart's equation[38], C-Sn-C bond angle can be calculated for the methyl and ethyl derivatives. The $^1J[^{119}Sn\text{-}^{13}C]$ values for the butyl and phenyltin(IV) derivatives were determined using the relationships proposed by Howard *et al.,*[42] and are given in Table 1.

3.3.3. ^{119}Sn NMR spectroscopy

According to literature the δ(^{119}Sn) values of four-coordinate complexes fall in the range +200 to −60 ppm; the five-coordinate complexes fall between −90 and −190 ppm, and the six- and seven-coordinate complexes fall between −210 and −400 ppm.[43] However, Chemical shifts δ (^{119}Sn) of six-coordinate chelate complexes lie in the range - 260 to - 404.6 ppm. The tin chemical shift δ (^{119}Sn) values indicated the coordination number of tin and thus provided the information about the geometry of organotin(IV) complexes. The δ (^{119}Sn) values were found to depend on the nature of the group attached to Sn. However, it must be carefully analyzed since tin resonance is strongly dependent upon other factors, such as electronegativity of the ligands, temperature and concentration employed in the experiments. In case of electron donating group the Sn atom becomes progressively more shielded and the δ (^{119}Sn) value moves to a higher field. The nature of the ligand (X) in organotin(IV) complexes ($R_{4-n}SnX_n$) also influence the values of δ (^{119}Sn). The electronegativity of the coordinating group of the ligand played a key role in the δ (^{119}Sn) value. Generally a higher electronegativity of the coordinate ligand shifts the δ (^{119}Sn) value to lower fields.[19,44]

The low field displacement of tin chemical shifts in case of R_3Sn (R = CH_3, C_2H_5 and C_4H_9) derivatives is caused by the influence of electron withdrawing and donating ability of the groups attached to ligand as well as electronegativity of the substituent at the tin atom. If the substituent has lone-pair electrons or π electrons of multiple bonds, then an increase in ^{119}Sn shielding will be observed due to the partial filling of the empty *5d* orbital of the tin atom (*d-p or* d_π-p_π interaction). The combination of these competitive effects leads to the tin shielding minimum for

the series $Sn(CH_3)_3$, $Sn(C_2H_5)_3$, $Sn(C_4H_9)_3$.[45,46] For complex **5**, Ph_3SnL, two peaks were observed, i.e., at -226.1 ppm and -257.7 ppm, respectively that represent the presence of the two species. The peak at -226.1 ppm may be due the presence of the 4-coordinate tetrahedral species while the other peak is due the presence of the 5-coordinate species. This was further conformed from the single crystal X-ray result in which the tin atom is present both in 4-coordinated as well as in 5-coordinated environments. In case of diorganotin(IV) derivatives the ^{119}Sn NMR values range from -271.7 ppm to -306.5 ppm falling in the range of 6-coordinate geometry. The ^{119}Sn NMR spectra of the complexes **1** and **4** are given in Figs. 1b and 1c, respectively.

Figs. 1a-1c

Table 1

3.4. X-Ray Crystallography

The perspective diagrams with unit cell packings for the complexes **1**, **3**, **4** are given in Figs. 2-7, respectively. Crystal data and structure refinement parameters are shown in Table 2 while the selected bond lengths and bond angles are given in Tables 3 and 4, respectively. The presence of a bidendate ligand, 4-(2-methoxy-5-nitrophenylamino)-4-oxobutanoate, leads to the formation of the polymeric structure. In other words, the central R_3Sn (R = CH_3 (**1**), C_4H_9 (**3**)) group bridges the two neighboring 4-(2-methoxy-5-nitrophenylamino)-4-oxobutanoate ligands *via* carboxylate moieties to form one-dimensional polymeric chain.[47] In complex **4** the geometry around the Sn atom is distorted tetrahedral due to steric hindrance of the three bulky phenyl groups. The values of τ ($\tau = (\beta-\alpha)/60$, where β is the largest basal angle around the tin atom while α is the next largest angle around the tin atom) for the complexes **1** and **3** are 0.87 and 0.92, respectively that are typical for distorted trigonal bipyramidal geometry.[48] The three R groups occupy the equatorial positions with essentially identical bond distances [Sn-C = 2.081-2.142 Å]. The O-Sn-O angle is approximately linear [O-Sn-O = 173.9-175.8°]. The C-Sn-C and O-Sn-C angles are within the expected range of values for 5-coordinated geometry around the tin atom [C-Sn-C = 114.4°-125.5° and O-Sn-C = 85.9-96.4°][49] for complexes **1** and **3**. The sum of the C-Sn-C angles in the equatorial plane equals 359.1° and 359.5°, respectively for complexes **1**and **3**, indicating slight distortion. This distortion from ideal trigonal bipyramidal geometry is found in the axial angle [O-Sn-O]. In case of complex **4** the C-Sn-C = 108.2°-114.9° that falls in the range of 4-coordinated tetrahedral geometry around the tin atom. In complex 4 two molecules are present in

the structure. However, when the structure of complex **4** was checked in Mercury software (Fig. 6c) then it was found that the Sn atoms are present in different environments, i.e., Sn1 is present in 5-coordinated environment while Sn2 in 4-coordinated environment. The bond distance of Sn1-O2 (2.605 Å) is longer than the normal Sn-O1 (2.054 Å) bond distance but due to weak interaction the O2 participate in coordination to Sn atom resulting in 5-coordinated geometry. The asymmetric Sn-O separations are reflected in the associated C1-O1 and C1-O2 distances of 1.276(9) Å, 1.236(9) Å and 1.258(8) Å, 1.258(8) Å, 1.210(2) Å, 1.224(6) Å, respectively for complexes **1** and **3**.[50] In this study complex **1** has a difference only 0.04 Å that is probably due the chelating nature of the carboxylate ligand. The anisobidentate bidentate carboxylate has a difference of 0.058 Å between its C-O bonds while for the bidentate carboxylate this difference is only 0.021 Å; the variations in the C-O bond distances suggest charge delocalization over the carboxylate group COO. The different modes of bonding of the acetates, i.e., bridging or chelating, are thus easily differentiated by the relevant bond lengths.[51] There is an intramolecular C-H---O interaction within the polymeric chain. Further, C-H---π interactions and intramolecular hydrogen bonds stabilize the polymeric chains in zigzag manner which are linked into a three-dimensional network *via* C-H---π interactions. The polar imino hydrogen atom of the amide derivative participates in intramolecular hydrogen bonds (N1-H1---O3). Complexes are self-assembled *via* π→ π, C-H---π and stacking interactions. Extended networks of O-Sn-O, C-H--O and C-H---π contacts lead to aggregation and a supramolecular assembly. The details of intramolecular H-bonds existing within the structure are given in Table 5.

Figures 2a-4c

Tables 2-5

3.4. Mass Spectrometry

Electrospray ionization (ESI) method was used to obtain the mass spectral data for the ligand and complexes. The data are given in the experimental section along with m/z and % intensity. The resultant fragments are in good agreement with the expected structures of the compounds. The general fragmentation patterns for tri- and diorganotin(IV) complexes are shown in Schemes 3 and 4, respectively

In the mass spectra of all the complexes, each fragment ion occurs in a group of peaks as a result of tin isotopes. For simplicity the mass spectral fragmentation data reported here are related to

the principal isotope ^{120}Sn.[52] The low-intensity molecular ion peaks, M^+ are observed in all synthesized organotin carboxylates (**1-10**). Also the $[MNa]^+$ Fragment is observed in all spectra. The fragmented ions are in good agreement with the expected structure of the compounds and consistent with the literature.[53,54]

In triorganotin compounds, three primary fragmentation patterns are proposed, based on observed m/z in their spectra. Elimination of different groups like COOR' and R, gave $[Sn]^+$ as end product in one of the pathways. The other two pathways after primary elimination of $[R]^+$ and $[R_3Sn]^+$ groups and then elimination of COO and successive R (in one of the pathway) results in the formation of $[R']^+$ (Scheme 4), which shows similar pattern for the further elimination of different groups.[55]

A bit different scheme of mass fragmentation pattern has been suggested for the diorganotin compounds (Scheme 5) but these pathways end up in similar manner as suggested for the triorganotin compounds. In addition, the following ions: $[C_4H_9]^+$, $[C_6H_5]^+$, $[C_7H_7]^+$, and $[C_8H_{17}]^+$ are also observed with reasonable intensities in the mass spectra of all organotin(IV) derivatives.[55]

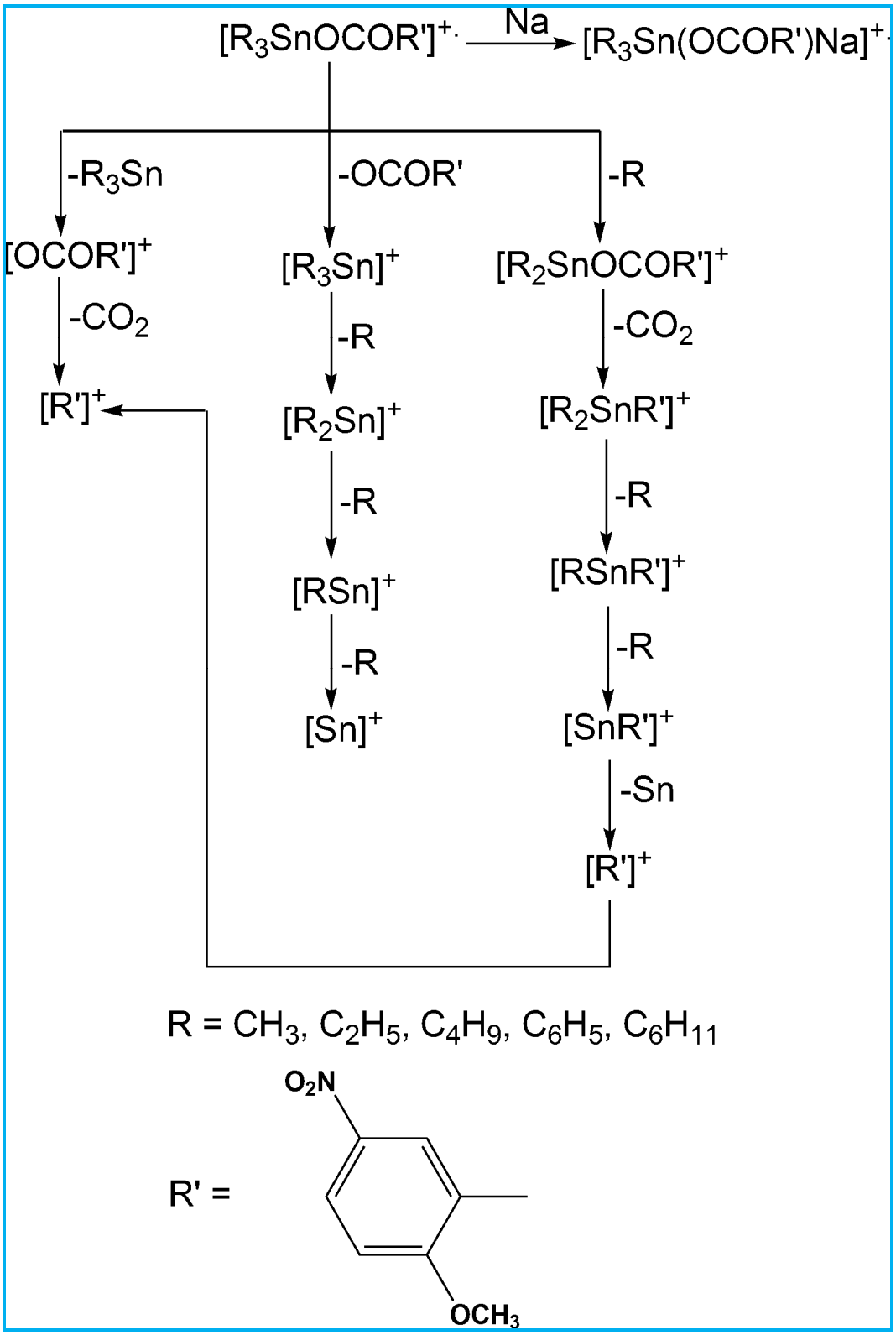

Scheme 4: General mass fragmentation pattern for triorganotin(IV) derivatives

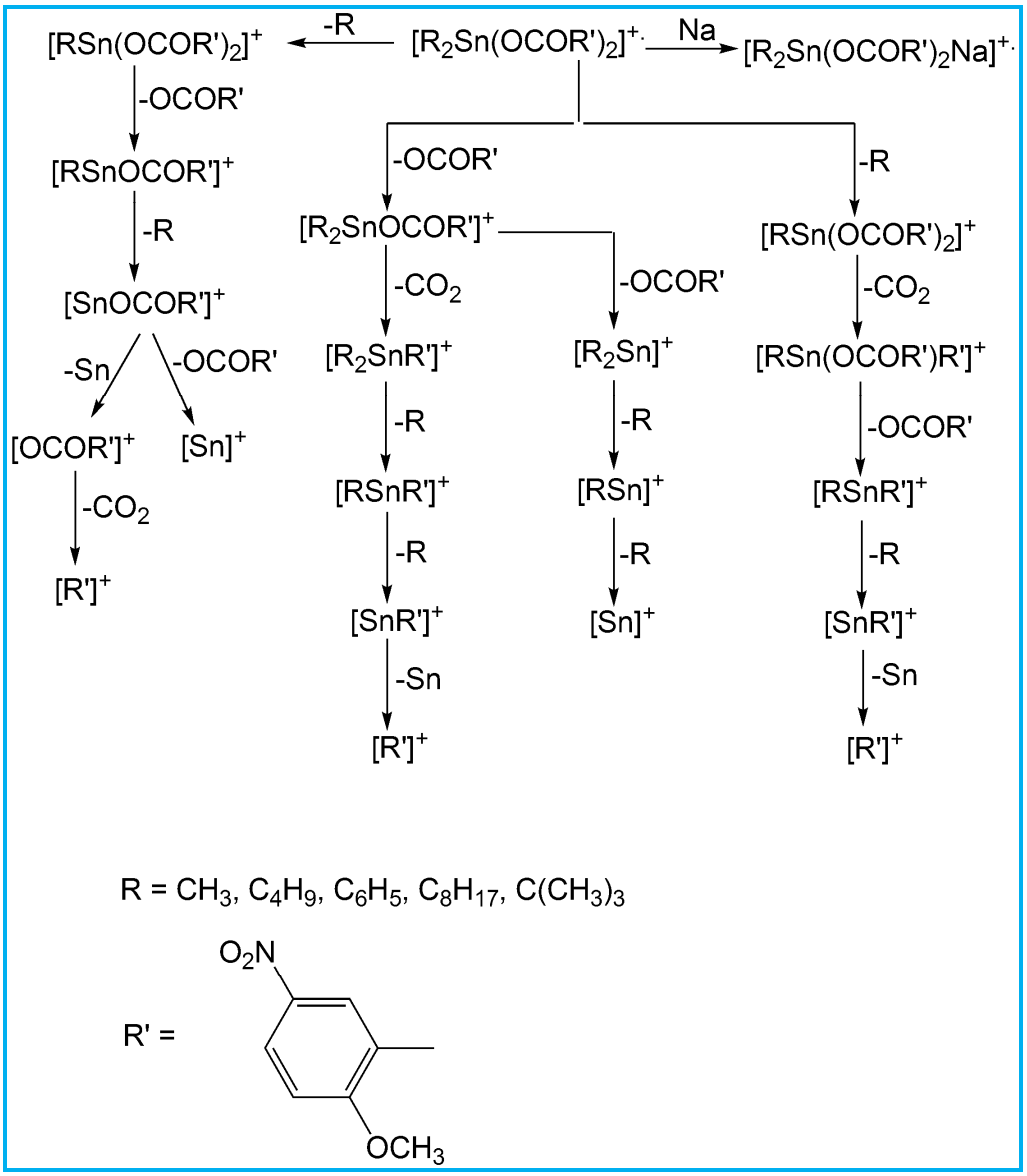

Scheme 5: General mass fragmentation pattern for diorganotin(IV) derivatives

3.7. Anticancer Activity

The mortality rate due to cancer is increasing worldwide due to the rapid growth of world population as well as adoption of cancer-causing behaviors. The search for the novel anticancer drugs continues. Agents that can eliminate the cancerous cells *via* a programmed cell death but do not affect the normal cells may have a therapeutic advantage for the elimination of cancer cells. In the present study, we provide evidence that investigated compounds act as a potential antiproliferative agent.[56] At present, only a few agents are known to possess the potential for selective/preferential elimination of cancer cells without affecting the normal cells.[57] The

discovery of *cis*-platin as an anticancer drug and recently its improved analogs (Carboplatin, Lobaplatin, Nedaplatin, Oxaliplatin) as marketing chemotherapeutic drugs give interest in exploration of metal-based anticancer drugs.[58]

The biological significance of the synthesized compounds is well renowned owing to their anticancer activity. Cytotoxicity evaluation of the investigated compounds explored another biological feature of the synthesized compounds as being strong anticancer agents. We examined the effects of the investigated compounds on the growth and proliferation of cancerous lung carcinoma (H-157) and kidney fibroblast (BHK-21) cell lines using an MTT assay to compare their behavior.[59] All the compounds showed remarkable cytotoxicity when checked at different concentrations. Vincristine was used as a standard drug and the IC_{50} values were shown in Table 6. The results revealed that all the tested compounds showed good cytotoxicity against H-157 and BHK-21 cell lines in a dose dependent manner. **NaL** demonstrated less cytotoxicity while compounds **1-5** exhibited moderate cytotoxic potency for both the cell lines. Compounds **6-10** showed good anticancer activity against both the cell lines and exhibited IC_{50} values near to standard drug, vincristine.

These results suggest that these compounds may be a good choice for cancer treatment after *in vivo* and other clinical studies. However, additional studies are needed to determine the exact mechanism(s) of apoptosis of the investigated compounds in cancer cells *versus* normal cells. Also, to establish a broader implication, additional studies are needed to verify these data in other normal cells and cancer cell types and to assess the effectiveness of the synthesized compounds in an *in vivo* model system.

Table 6

3.8. Antileishmanial activity

MTT assay was used to examine the *in vitro* antileishmanial activity of the synthesized compounds against the promastigote forms of leishmania major. The investigated compounds produced a significant reduction in viable promastigotes as shown in Table 7. All the synthesized compounds exhibit strong antileishmanial activity when checked at different concentrations. Amphotericin B was used as standard. The IC_{50} values shown in Table 7 revealed that compound **10** was the most potent against promastigote forms of leishmania major and exhibited IC_{50} value 0.98 ± 0.06 μM as compared to amphotericin B which represent IC_{50} value 0.29 ± 0.05 μM.

Compounds **7-9** also showed remarkable potency against leishmanias, while rest of the compounds exhibited moderate antileishmanial activity. Their antileishmanial activity may be due the interference with the function of parasite mitochondria. This study, therefore, demonstrated the potential use of these compounds as source of novel agents for the treatment of *leishmaniasis*.

Table 7

3.5. DNA binding study by UV-Visible spectroscopy

Electronic absorption spectra were initially used to examine the interaction between the compounds and SS-DNA. Figures **7-11** show the UV-visible spectra observed when representative compound's (**1**, **2**, **3**, **4** and **7**) interact with different concentrations of DNA. It was observed that all compounds except **7** have two strong absorption peaks at 254-257.6 nm and 291.80-296.40 nm which are probably due to π-π* (due to aromatic group) and n-π* (either due to NO_2 or CO groups) transitions, respectively. In case of compound **7** a strong absorption peaks at 439.50 nm is appeared. After interaction with increasing amounts of DNA, all the peaks decreased gradually (means having hypochromic effect) and there was a minor red shift of upto 5 nm for all compounds. Long *et al*.,[60] have pointed out that the peak shift of the small molecules after they interacted with DNA could be clues to judge the binding mode between the small molecules and DNA: If the binding involves a typical intercalative mode, an hypochromism effect coupled with obvious bathochromism for the characteristic peaks of the small molecules will be found due to the strong stacking between the chromophore and the base pairs of DNA.[61] Therefore, based on this viewpoint, the interaction between compounds and SS-DNA could be noncovalent intercalative binding. After intercalating the base pairs of DNA, the π* orbital of the intercalated ligand could couple with π orbital of base pairs, thus decreasing the π-π* transition energy, and further resulting in the bathochromism. On the other hand, the coupling of a π orbital with partially filled electrons decreases the transition probabilities hence results hypochromic shift. Since hypochromism due to π-π* stacking interactions may appear in the case of the intercalative binding mode, while bathochromism (red-shift) may be observed when the DNA duplex is stabilized.[62] The stability of the DNA-compound complex was also checked after 24 h and 48 h and got the same result which means that the DNA-compound complex is stable.

Based upon the variation in absorbance, the intrinsic binding constant of the compound with DNA were determined according to Benesi-Hildebrand's equation[63]:

$$\frac{A_0}{A-A_0} = \frac{\varepsilon_G}{\varepsilon_{H-G}-\varepsilon_G} + \frac{\varepsilon_G}{\varepsilon_{H-G}-\varepsilon_G} \times \frac{1}{K[DNA]}$$

where *K* is the association/binding constant, A_o and A are the absorbances of the compound and its complex with DNA, respectively, and ε_G and ε_{H-G} are the absorption coefficients of the compound and the compound-DNA complex, respectively. The association constants were obtained from the intercept-to-slope ratios of $A_o/(A-A_o)$ *vs.* 1/[DNA] plots. The Gibb's free energy (ΔG) was determined from the equation:

$$\Delta G = -RT \ln K$$

where R is general gas constant (8.314 $JK^{-1}.mol^{-1}$) and T is the temperature (298 K). The values of *K* and ΔG are given in the inset graph of the corresponding figures. The order of interaction with DNA is as: **2 > 1 > 3 > 4 ~ 7**.

DNA and enzymes represent the most targeted bioreceptors for small molecules as various regulatory processes such as gene expression, gene transcription, mutagenesis, carcinogenesis.[64] Most anticancer drugs bind to DNA and proteins either in a reversible or irreversible manner suggesting a direct relationship between their interactions with macromolecules, hence, leading to their therapeutic effect.[65] It was proposed that the compounds interact with nitrogenous bases of nucleotides of nucleic acid and inhibit the cell division by interfering the replication and transcription of DNA molecules. The compounds may also affect the multienzyme complexes responsible for replication and transcription of DNA thus causing a stop of proliferation of the cells.[66] From the interaction study with SS-DNA it can be concluded that the synthesized compounds may be used as an anticancer drug.

Figures 7-11

4. Conclusions

Sodium salt of N-[(2-methoxy-5-nitrophenyl)]-4-oxo-4-[oxy]butanamide was obtained in good yield and was characterized by FT-IR. Multinuclear NMR results showed that triorganotin(IV) derivatives exhibit distorted trigonal-bipyramidal both in solution and solid states. While in the case of diorganotin(IV) derivatives the proposed geometry around the tin atom is octahedral. A good correlation was found between the Δν value calculated from the FT-IR data and the single

crystal XRD data. From the single crystal X-ray structural analysis it is revealed that these compounds have packing diagrams like dendrimers with characteristics that make them useful for numerous biological applications. The synthesized compounds exhibited significant cytotoxic and antileishmanial activity. These results may lead to development of new drug against cancer cells and leishmanias after *in vivo* studies. Binding studies of small molecules to DNA are very important in the development of DNA molecular probes and new therapeutic reagents. UV-visible spectroscopic results show that the synthesized compounds bind to DNA *via* intercalative mode of interaction resulting in hypochromism and minor red shift.

Supplementary material

Crystallographic data for complexes **1**, **3** and **4** reported in this paper have been deposited with the Cambridge Crystallographic Data Centre, CCDC# 984493, 984494 and 984495 and for complexes **1**, **3** and **4**, respectively. Copies of this information may be obtained free of charge from The Director, CCDC, 12, Union Road, Cambridge CB2 1EZ [Fax: +44 1223 336 033] or deposit@ccdc.cam.ac.uk or http://www.ccdc.cam.ac.uk.

Acknowledgment

M. Sirajuddin gratefully acknowledges the Higher Education Commission (HEC) Islamabad, Pakistan, for financial support.

References

[1] Garza-Ortiz, C. Camacho-Camacho, T. Sainz-Espunes, I. Rojas-Oviewedo, L.R. Gutierrez-Lucas, A.G. Carrillo, M.A.V. Ramirez, *Bioinorg. Chem. Appl*., 2013, 2013, 1–12.

[2] S. Roy, K.D. Hagen, P. U. Maheswari *et al*., *Chem. Med. Chem*., 2008, 3, 1427–1434.

[3] L. Pellerito and L. Nagy, *Coord. Chem. Rev*., 2002, 224, 111–150.

[4] S. Tabassum, M. Afzal, F. Arjmand, *Eur. J. Med. Chem*., 2013, xxx, 1–9.

[5] A. Alama, B. Tasso, F. Novelli, F. Sparatore. *Drug Discovery Today*, 2009, 14, 500–508.

[6] I. Ott, R. Gust, *Arch. Pharm. Chem. Life Sci*., 2007, 340, 117–126.

[7] M. Gielen, *Appl. Organomet. Chem*., 2002, 16, 481–494.

[8] M. Nath, S. Pokharia, R. Yadav, *Coord. Chem. Rev*., 2001, 215, 99–149.

[9] P. Desjeux, *Trans. R. Soc. Trop. Med. Hyg*., 2001, 9, 239–243.

[10] H.W. Murray, Agents Chemother., 2001, 45, 2185–2197.

[11] P. Marty, E. Rosenthal, Expert Opin. Pharmacother., 2002, 3, 1101–1108.

[12] B.L. Herwaldt, J.D. Berman, Am. J. Trop. Med. Hyg., 1992, 46, 296–306.

[13] S. Sundar, Trop. Med. Int. Health, 2001, 6, 849–854.

[14] S.L. Croft, G.H. Coombs, Trends Parasitol., 2003, 19, 502–508.

[15] B. Raychaudhury, S. Banerjee, S. Gupta, R.V. Singh, S.C. Datta, *Acta Tropica*, 2005, 95, 1–8.

[16] W.L.F. Armarego, C.L.L. Chai, in "Purification of Laboratory Chemicals", 5th Edn., Butterworth-Heinemann, London, New York, (2003).

[17] G.M. Sheldrick, *Acta Cryst*., 2008, A64, 112–122.

[18] G.M. Sheldrick, University of Göttingen, Germany (2012).

[19] M. Sirajuddin, S. Ali, V. McKee, M. Sohail, H. Pasha, *Eur. J. Med. Chem*., 2014, 84, 343–363.

[20] K. Araki-Sasaki, S. Aizawa, M. Hiramoto, M. Nakamura, O. Iwase, K. Nakata, Y. Sasaki, T. Mano, H. Handa, Y. Tano, *J. Cell Physiol*., 2000, 182, 189–195.

[21] P. Skehan, R. Storeng, D. Scudiero, A. Monks, J. McMahon, D. Vistica, J.T. Warren, H. Bokesch, S. Kenney, M.R. Boyd, *J. Natl. Cancer Inst*., 1990, 82, 1107–1112.

[22] G.S. Longo-Sorbello, G. Saydam, D. Banerjee, J.R. Bertino, Cytotoxicity and cell growth assays. Cell Biology, Four-Volume Set: A Laboratory Handbook, 2005, 1, 315.

[23] T. Mosmann, *J. Immunol. Methods*, 1983, 65, 55–63.

[24] M. Niks, M. Otto, *J. Immunol. Methods*, 1990, 130, 149–151.

[25] M. Tariq, S. Ali, N. Muhammad, N.A. Shah, M. Sirajuddin, M.N. Tahir, N. Khalid, M.R. Khan, *J. Coord. Chem*., 2014, 67, 323–340.

[26] M. Sirajuddin, S. Ali, A. Badshah, *J. Photochem. & Photobiology B*, 2013, 124, 1–19.

[27] M. Sirajuddin, Nooruddin, S. Ali, M.N. Tahir, *Spectrochim. Acta Part A*, 2013, 116, 111–121.

[28] M. Sirajuddin, S. Ali, F.A. Shah, M. Ahmad, M.N. Tahir, *J. Iran. Chem. Soc*., 2014, 11, 297–313.

[29] F.W. Yip, Y. Farina, S.G. Teoh, S.H. Inayat-Hussain, B.M. Yamin, I. Baba, A.M. Ali, Malaysian *J. Pharm. Sci*., 2006, 4, 33–47.

[30] D. Kovala-Demertzi, V.N. Dokorou, J.P. Jasinski, A. Opolski, J. Wiecek, M. Zervou, M.A. Demertzis, *J. Organomet. Chem*., 2005, 690, 1800–1806.

[31] J. Li, G. Zhao, G. Xiong, Y. Ma, Synth. React. Inorg. Met.-Org. Chem., 31, 2001, 85–93.

[32] M. Nara, H. Torii, M. Tasumi, *J. Phys. Chem*., 1996, 100, 19812–19817.

[33] V. Zelenak, Z. Vargova, K. Gyoryova, Spectrochim. Acta Part A, 2007, 66, 262–272.

[34] E. Yousif, *J. King Saud Univ. Sci*., 2012, 24, 167–170.

[35] J. Holecek, M. Nadvornik, K. Handlir, A. Lycka, *J. Organomet. Chem*., 1986, 315, 299–308.

[36] T.P. Lockhart, W.F. Manders, *Inorg. Chem*., 1986, 25, 892–895.

[37] Y. Farina, A. Graisa, E. Yousif, *Mod. Appl. Sci*., 2009, 3, 215–218.

[38] T.P. Lockhart, W.F. Manders, E.M. Holts, *J. Am. Chem. Soc*., 1986, 108, 6611-6616.

[39] B. Wrackmeyer, *Annu. Rep. NMR Spectrosc*., 38, 1999, 203–264.

[40] A. Lycka, M. Nadvornik, K. Handlir, J. Holecek, *Collect. Czech. Chem. Commun*., 1984, 49, 2903–2911.

[41] R. Willem, A. Bouhdid, M. Biesemans, J.C. Martins, D. Vos, E.R.T. Tiekink, M. Gielen, *J. Organomet. Chem*., 1996, 514, 203–212.

[42] W.F. Howard, R.W. Crecely, W.H. Nelson, Inorg. Chem., 1985, 24, 2204–2208.

[43] J. Holecek, M. Nadvorník, K. Handlir, A. Lycka. *J. Organomet. Chem*., 315 (1986) 299–308.

[44] H. Masood, S. Ali, M. Mazhar, S. Shahzadi, K. Shahid, *Turk. J. Chem*., 2004, 28, 75–85.

[45] V.N. Torocheshnikov, A.P. Tupciauskas, A.Y. Ustynyuk, *J. Organomet. Chem*., 1974, 81, 351–356.

[46] J.J. Burke, P.C. Lauterbur, *J. Am. Chem. Soc*., 1961, 83, 326–331.

[47] A.W. Addison, R.T. Nageswara, J. Reedijk, J. Van Rijn, G.C. Verschoor, *J. Chem. Soc. Dalton Trans*., 1984, 1349–1356.

[48] M.N. Tahir, D. Ulku, M. Danish, S. Ali, A. Badshah, M. Mazhar, *Acta Cryst*., 1997, C53, 183–185.

[49] Sadiq-ur-Rehman, S. Ali, M. Mazhar, M. Parvez, *Acta Cryst*., 2004, E60, m1394–m1396.

[50] T.S.B. Baul, E.R.T. Tiekink, *Acta, Cryst*., 1996, C52, 1428–1430.

[51] V. Dokorou, M.A. Demertzis, J.P. Jasinski, D. Kovala-Demertzi, *J. Organomet. Chem*., 2004, 689, 317–325.

[52] Sadiq-ur-Rehman, K. Shahid, S. Ali, M.H. Bhatti, M. Parvez, *J. Organomet. Chem*., 2005, 690, 1396–1408.

[53] M.H. Bhatti, S. Ali, M. Mazhar, M. Danish, M.A. Choudhary, Turk. J. Chem., 1999, 23, 329–337.

[54] S. Shahzadi, K. Shahid, S. Ali, M.H. Bhatti, *J. Chem. Soc. Pak*., 2004, 26, 395–399.

[55] Sadiq-ur-Rehman, M.A. Choudhary, M.H. Bhatti, S. Ali, *J. Iran. Chem. Soc*., 2012, 9, 35–45.

[56] N. Ahmad, D.K. Feyes, A.L. Nieminen, R. Agarwal, H. Mukhtar, *J. Natl. Cancer Inst*., 1997, 89, 1881–1886.

[57] R. Raza, A. Matin, S. Sarwar, M. Barsukova-Stuckart, M. Ibrahim, U. Kortz, J. Iqbal, *Dalton Trans*., 2012, 41, 14329–14336.

[58] Y.F. Win, C.S. Choong, J.C. Dang, M.A. Iqbal, C.K. Quah, A.M.S.A. Majid, S.G. Teoh, *J. Coord. Chem*., 67 (2014) 3401–3413.

[59] S.K. Shukla, V.K. Tiwari, R. Sushma, I.C. Tewari, *J. Med. Chem. Lett*., 2011, 1, 10–19.

[60] E.C. Long, J.K. Barton, *Chem. Res*., 1990, 23, 271–273.

[61] M. Sirajuddin, S. Ali, A. Haider, N.A. Shah, A. Shah, M.R. Khan, *Polyhedron*, 2012, 40, 19–31.

[62] M. Sirajuddin, S. Ali, N.A. Shah, M.R. Khan, M.N. Tahir, *Spectrochim. Acta Part A*, 2012, 94, 134–142.

[63] H.A. Benesi, J.H. Hildebrand, *J. Am. Chem. Soc*., 1949, 71, 2703–2707.

[64] R. Palchaudhuri, P.J. Hergenrother, *Curr. Opin. Biotechnol*., 2007, 18, 497–503.

[65] L.H. Hurley, *Nat. Rev. Cancer*, 2002, 2, 188–200.

[66] N. Ahmad, S. Gupta, M.M. Husain, K.M. Heiskanen, H. Mukhtar, *Clin. Cancer Res*., 2000, 6, 1524–1528.

Graphical Abstract

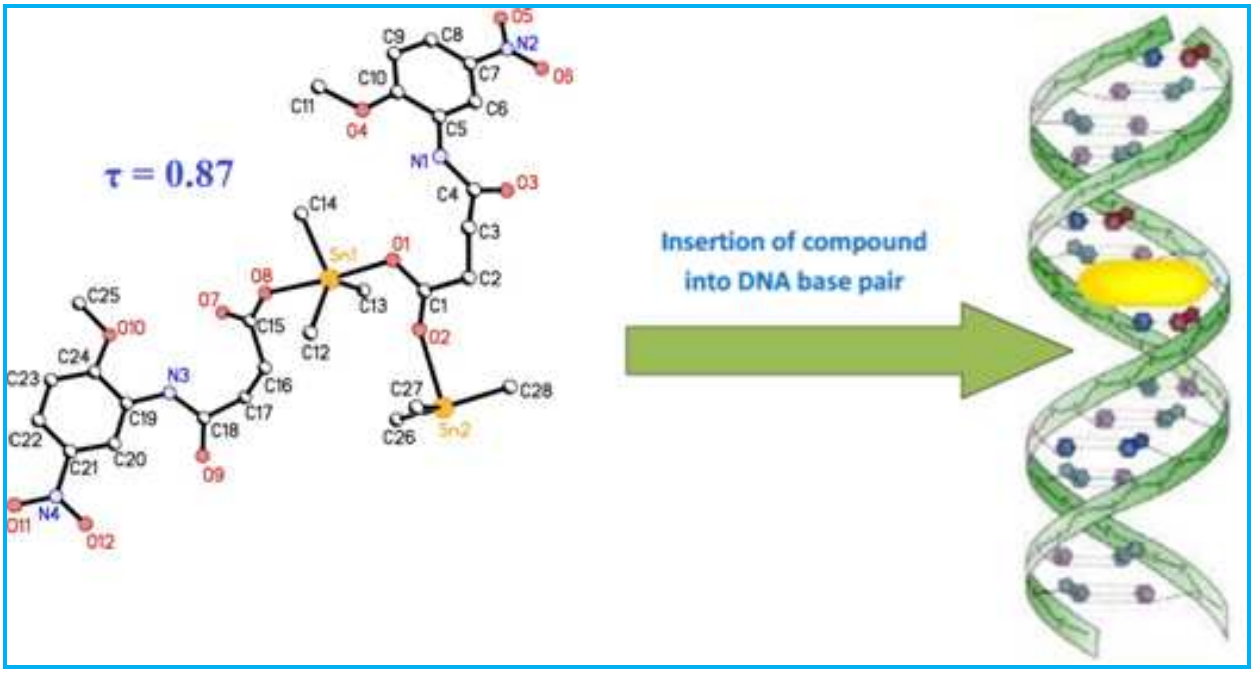

Synopsis for graphical abstract

The compounds interact with DNA *via* intercalative mode of interaction. They show strong antibacterial, anticancer and antileishmanial activities.